NANO LETTERS

Letter

pubs.acs.org/NanoLett

Fabrication of Nanoassemblies Using Flow Control

Chad Ropp,[†] Zachary Cummins,[‡] Sanghee Nah,[§] Sijia Qin,[§] Ji Hyun Seog,[⊥] Sang Bok Lee,[⊥,§] John T. Fourkas,*[,§,∥] Benjamin Shapiro,*[,‡,#] and Edo Waks*[,†]

[†]Department of Electrical and Computer Engineering/IREAP, [#]The Institute for Systems Research, [‡]Fischell Department of Bioengineering, [§]Department of Chemistry and Biochemistry, and [∥]Institute for Physical Science and Technology, University of Maryland, College Park, Maryland 20742, United States

[⊥]Graduate School of Nanoscience and Technology (WCU), KAIST, 335 Gwahak-ro, Yuseong-Gu, Daejeon, 305-701, Korea

Supporting Information

ABSTRACT: Synthetic nanostructures, such as nanoparticles and nanowires, can serve as modular building blocks for integrated nanoscale systems. We demonstrate a microfluidic approach for positioning, orienting, and assembling such nanostructures into nanoassemblies. We use flow control combined with a cross-linking photoresist to position and immobilize nanostructures in desired positions and orientations. Immobilized nanostructures can serve as pivots, barriers, and guides for precise placement of subsequent nanostructures.

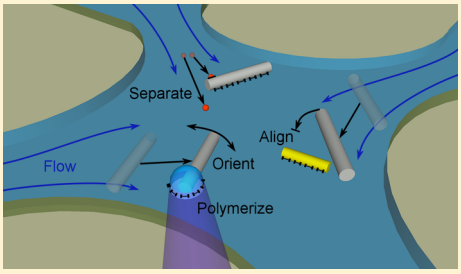

KEYWORDS: *Nanofabrication, quantum dots, nanowires, microfluidics, electroosmotic flow*

Nanosystem engineering paves a pathway toward inexpensive[1] and high bandwidth[2] nanoelectronics, subwavelength photonics,[3] ultrasensitive biological detectors,[4] customizable metamaterials,[5] and quantum circuits.[6] These applications require controlled interactions among different nanostructures such as quantum dots,[7] nanowires,[8] and plasmonic nanoantennas.[9,10] Nanostructures can be prepared by solution-phase chemistry with high uniformity and superb properties. However, integrated devices require the ability to assemble individual components in specific geometries with nanoscale precision. On-chip assembly approaches that rely on random deposition can assemble small-scale devices with a few interacting components.[9−11] However, these approaches suffer from low device yield, especially when constructing larger systems with many components. Deterministic assembly methods overcome this problem by positioning preselected nanostructures at desired locations on demand.

Deterministic assembly relies on the ability to manipulate nanostructures with nanoscale precision. Optical tweezers can manipulate[12] and assemble[13−15] nano and microscale structures in three dimensions using optical gradient forces that are proportional to the structure's polarizability. Because polarizability scales with volume, optical manipulation of nanoscale structures is challenging.[16] Magnetic tweezers[17] or dielectrophoretic actuation[18] can also manipulate nanostructures, but these methods apply forces that also scale with volume. Mechanical tips have been used to drag or push nanostructures along a surface and position them with nanoscale precision.[19] This technique requires complex stabilization and control that is highly dependent on both the material composition of the nanostructure and the properties of the surface.[20] Mechanical forces can also damage the positioned nanostructure.[21]

Flow control is an alternate strategy for positioning nanostructures along a surface.[22,23] This approach uses fluid flow in a microfluidic device to move structures suspended in the fluid.[24] A feedback control system tracks an individual nanostructure in real time and continuously actuates flow to correct its position, which can be controlled with 39 nm precision.[23] This precision is insensitive to the composition or size of the structure and is determined primarily by the tracking precision and the accuracy of the control algorithm. Flow control can also manipulate a broad range of structures including fluorescent molecules,[25,26] quantum dots,[22,23,25,27] nanowires,[28] and live cells.[29] This versatility is vital for assembling nanosystems composed of many different materials using a single manipulation platform.

Here we demonstrate the use of flow control within an aqueous photoresist for the sequential positioning and immobilization of individual nanostructures to form nanoassemblies. We develop a toolbox of capabilities for positioning, orienting, and immobilizing nanostructures. We use obstructions in the microfluidic device as pivots, barriers, and guides to orient, separate, and combine multiple nanostructures. Once a nanostructure is positioned and oriented, we immobilize it by locally polymerizing the surrounding photoresist with UV illumination. As a demonstration of the scalability of the approach, we create nanoassemblies composed of multiple silver nanowires.

Figure 1A shows an optical image of the flow control device used to manipulate nanostructures and create nanoassemblies.

Received: June 6, 2013
Revised: July 18, 2013
Published: July 24, 2013

dx.doi.org/10.1021/nl402059u | *Nano Lett.* 2013, 13, 3936−3941

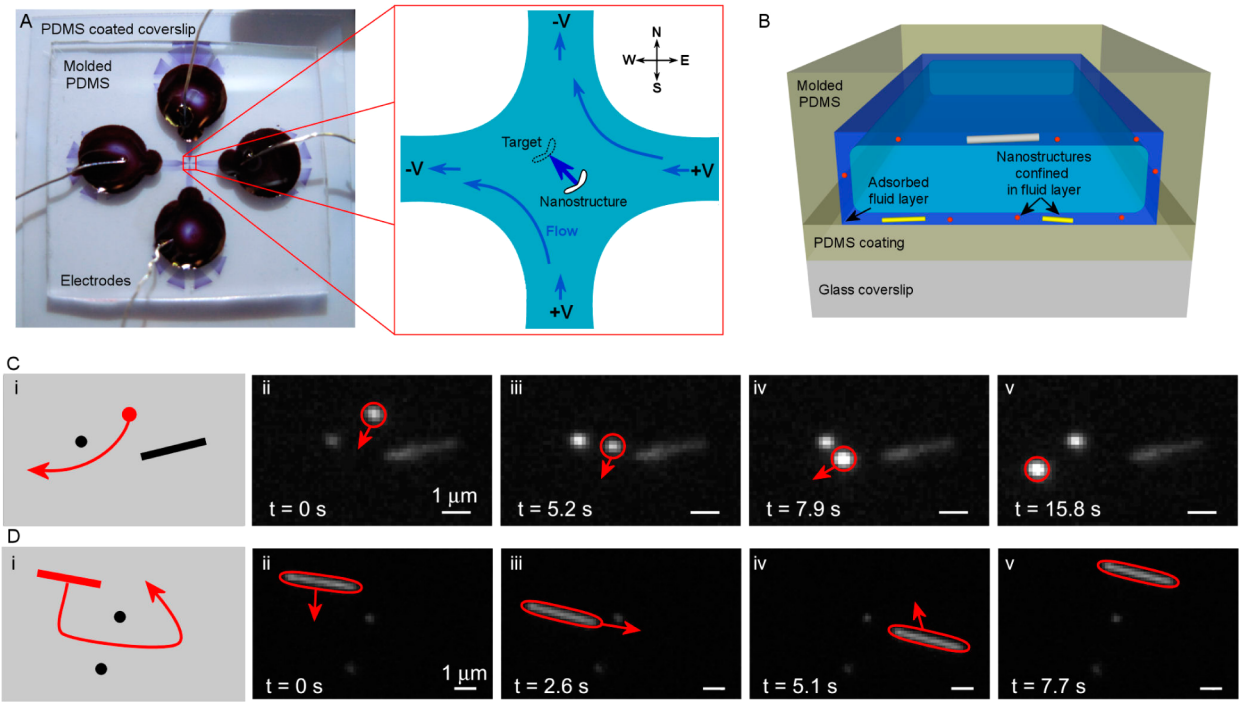

Figure 1. (A) Optical image of the microfluidic device. Channels are formed from molded PDMS placed on top of a PDMS-coated coverslip. Reservoirs are cut from the PDMS to access the channels (here filled with a dark fluid). Electrodes placed in the reservoirs actuate electroosmosis. The expanded region corresponds to the control chamber in the center of the cross channel. Voltages applied to the four electrodes create electroosmotic flow to move a nanostructure in any desired direction within the control chamber. (B) Schematic side view of the microfluidic channel depicting the fluid layers that confine nanostructures to the device surfaces. The microfluidic device is 5 μm high and the fluid layer is approximately 100 nm thick. (C) (i) Schematic of quantum dot steering between two nanostructures adhered to the device surface (ii–v) Time-stamped images of the steering process. Arrows denote the direction of fluid flow. (D) (i) Schematic of silver nanowire steering between two nanostructures on the surface. (ii–v) Time-stamped images of the steering process. Arrows denote direction of fluid flow.

The device consists of two orthogonal microfluidic channels that intersect to form a control chamber (indicated by the red box). We mold channels in polydimethylsiloxane (PDMS) and place them on top of a PDMS-coated coverslip. The control chamber is approximately 100 μm in diameter and 5 μm in height. Electrodes placed in the four channel reservoirs actuate electroosmotic flow[30] within the control chamber along the four cardinal directions (North, South, East, and West).[29] We actuate flow to move a suspended nanostructure in any desired direction by applying a combination of these four voltages, as illustrated in the red zoom-out box. To achieve nanoscale positioning, we use feedback control, which tracks the position of a suspended nanostructure in real time using an image centroiding algorithm.[31] The measured position serves as an input to a feedback controller that creates correcting flow to move to and maintain the nanostructure at a desired location.[29]

Flow control positions nanostructures along the plane of the chip surface. To prevent nanostructures from diffusing out-of-plane, we use a specialized fluid chemistry (previously reported in ref 22) that confines them to within 100 nm of the surface of the device, as depicted in Figure 1B. The control fluid is an aqueous solution containing a partially miscible acrylic monomer resin (SR-9035, Sartomer). We manipulate nanostructures in-plane on either the top or bottom of the device. The fluid also contains a rheology modifier (Acrysol RM-825, Rohm and Haas Co.)[32] that increases viscosity to reduce Brownian motion, as well as a zwitterionic betaine surfactant (EDAB)[33] that improves electroosmotic actuation along the PDMS surfaces. The fluid is composed of 40–52.5% by volume monomer resin, 1.31–0.83 wt % rheology modifier and 0.30 wt % EDAB. It also contains 0.5 wt % of a water-soluble photoinitiator.[34] The photoresist polymerizes when exposed to UV light to immobilize nanostructures within the locally exposed region.[22] We polymerize the photoresist using a 375 nm UV laser focused through the bottom glass coverslip.

We perform all measurements using an inverted microscope system. An oil-immersion objective with an NA of 1.45 images nanostructures suspended in the control chamber, while an EMCCD camera acquires images at a 10 Hz frame rate. The control algorithm uses the acquired images to calculate the centroid position of the nanostructure and to adjust the voltages applied to the microfluidic device accordingly. We image nonfluorescent nanostructures using white-light illumination. Fluorescent nanostructures are imaged by exciting with a 532 nm laser source and focusing the collected emission to the camera.

We first demonstrate steering of colloidal quantum dots and silver nanowires. We use commercially available CdSe/ZnS quantum dots (Ocean Nanotech) and silver nanowires that we synthesize by reducing $AgNO_3$ with ethylene glycol, using a procedure modified from ref 35. The quantum dots are mixed in with the fluid while silver nanowires are locally deposited onto the device surface prior to filling. Some of the deposited nanowires detach from the surface and become suspended when the device is filled with fluid. Figures 1C and 1D are series of optical images showing manipulation of a single quantum dot and a single silver nanowire, respectively (see Supporting Information Videos si_002 and si_003). Figure 1C shows a single quantum dot steered between a quantum dot and a silver nanowire that are immobilized to the surface.

dx.doi.org/10.1021/nl402059u | *Nano Lett.* 2013, 13, 3936–3941

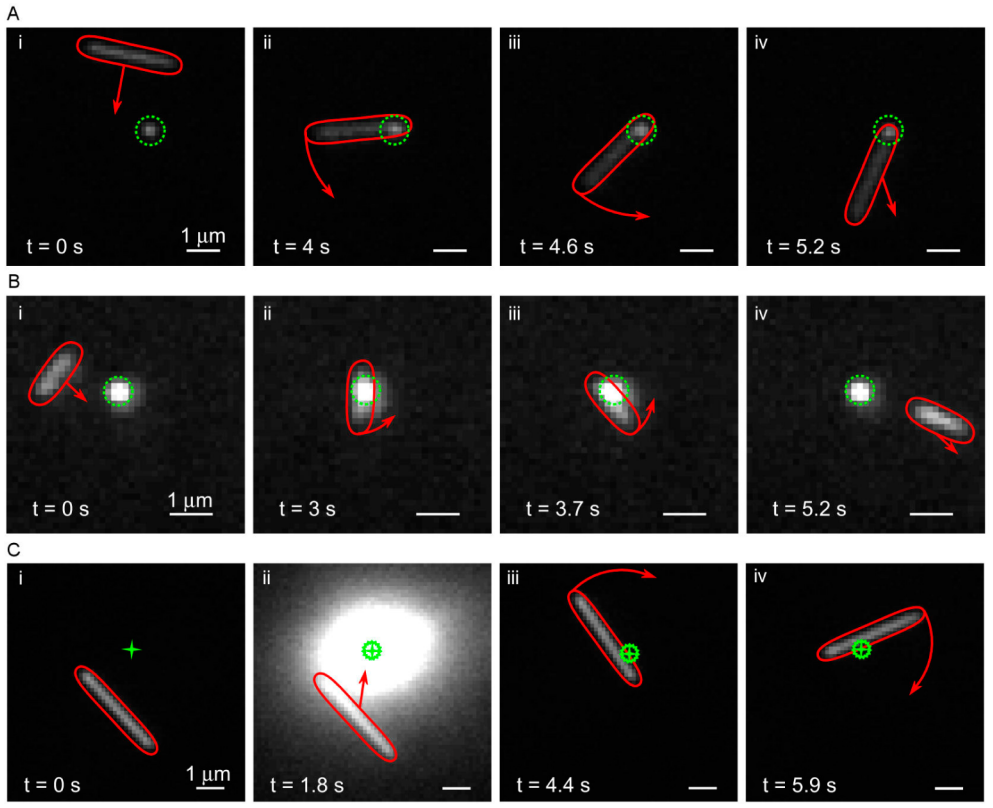

Figure 2. (A) Time-stamped images illustrating rotation of a silver nanowire using a nanoscale pivot. (B) Time-stamped images illustrating rotation of a gold nanowire using a nanoscale pivot. (C) Time-stamped images illustrating rotation of a silver nanowire using a polymerized pivot created by UV exposure. The green crosshairs denote the location of the UV focal spot. In all figures, the arrows denote direction of nanostructure translation and rotation and green circles indicate the location of the pivot.

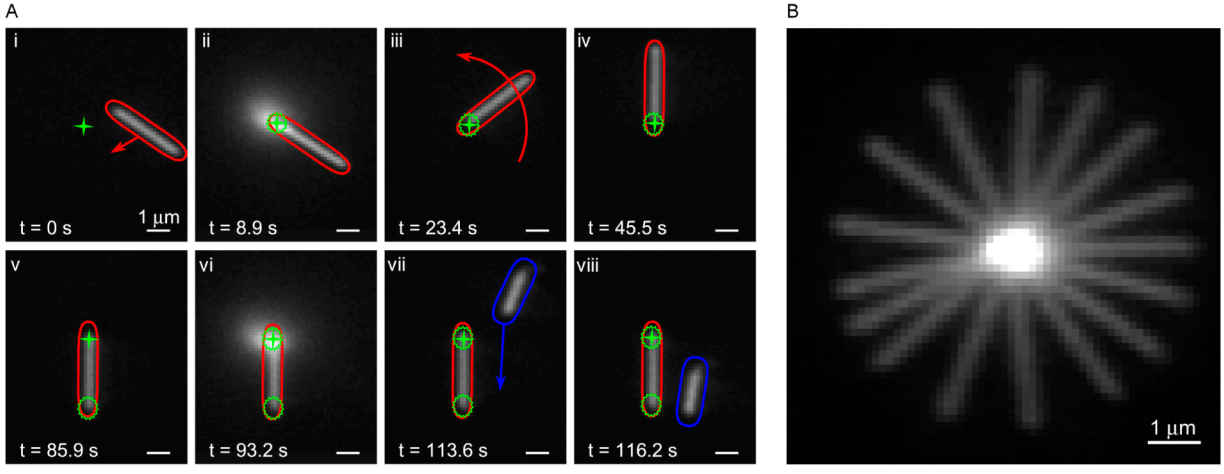

Figure 3. (A) Orienting a silver nanowire by immobilizing one end. (i) The nanowire is positioned so that its end is at the focus (green crosshair) of the UV laser. (ii) Local UV exposure immobilizes one end of the nanowire. (iii,iv) The nanowire is rotated about the immobilized end and held at a vertical orientation. (v) The stage is translated so that the UV focus is at the free end of the nanowire. (vi) A second UV exposure immobilizes the second end of the nanowire. (vii,viii.) Subsequent actuation of fluid flow confirms that the nanowire is immobilized, as is seen from the motion of a second silver nanowire (blue). (B) Composite image from several frames of a silver nanowire rotating 360° about its immobilized end.

Figure 1D shows a silver nanowire steered between two silver nanoparticles that are immobilized to the surface. In both cases, all three nanostructures were in the same focal plane, indicating that they were all at the surface of the device.

In previous work, we used flow control to position quantum dots with 39 nm precision.[23] Here we show that flow control can position silver nanowires with significantly better precision. We determine this precision by holding a silver nanowire in place and continuously monitoring its centroid position for 60 s. From the measured positions, we find the standard deviation of the wire position to be σ_p = 5 and 3 nm in the directions perpendicular to and parallel to the wire axis. These numbers are corrected for noise in the tracking algorithm, which we determine by tracking a stationary wire that is immobilized on the sample surface (see Supporting Information).

dx.doi.org/10.1021/nl402059u | *Nano Lett.* 2013, 13, 3936−3941

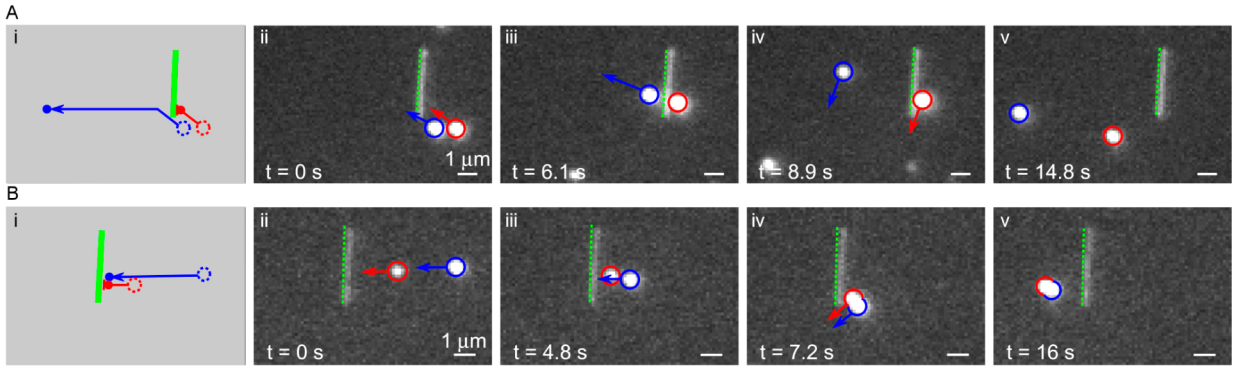

Figure 4. (A) (i) Quantum dot separation (blue from red) using a silver nanowire barrier. (ii–v) Time-stamped images of the separation. (B) (i) Combining two quantum dots (blue to red) using a silver nanowire barrier. (ii–v) Time-stamped images. In all panels the arrows denote direction of particle motion and green delineates the location of the barrier.

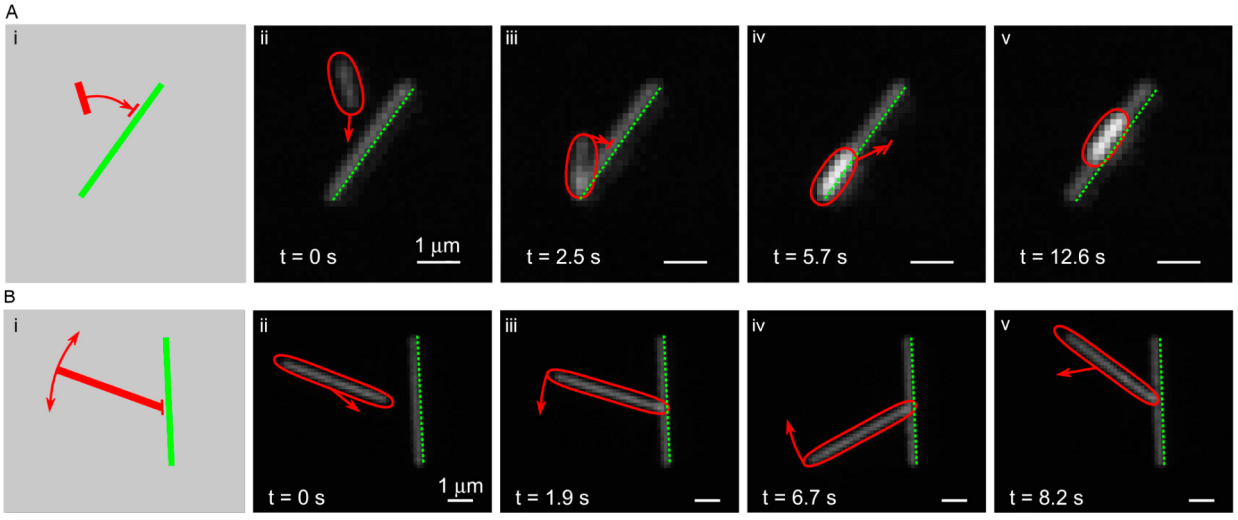

Figure 5. (A) (i) Alignment of a gold nanowire to an immobilized silver nanowire guide. (ii–v) Time-stamped images of the alignment process. (B) (i) Silver nanowire rotation using a second immobilized silver nanowire barrier. (ii–v) Time-stamped images of the rotation. In all panels, the arrows denote direction of fluid flow and object rotation and green delineates the location of the immobilized nanowire.

In addition to its centroid position, we also need to control the orientation of the nanowire. Optical[36] and magnetic[37] fields can rotate nanostructures to desired angles, but the applied torque depends on the nanostructure's polarizability or magnetization, respectively. Flow control can rotate nanostructures independently of their material properties by taking advantage of shear flows.[28] However, this type of manipulation requires a more complex control algorithm and has only been demonstrated previously for wires with lengths exceeding 10 μm. Here we use flow control in combination with immobilized nanostructures that serve as pivots for orienting wires. This approach takes advantage of the confinement of nanostructures to a thin fluid layer near the device surface (Figure 1B). Our method requires only a simple control algorithm, and can control the orientation of wires as short as 1 μm.

Nanostructures are first deposited onto the device surface and they immobilize before the channels are filled with fluid. Figure 2 shows several image sequences that demonstrate the rotation of a gold or silver nanowire using an immobilized pivot (see Supporting Information Videos si_004, si_005, and si_006). We rotate the wire by pressing one of its ends against the pivot and applying a perpendicular flow. In row A, a silver nanowire (3 μm long) rotates about a pivot composed of a silver nanoparticle (indicated by a dashed circle). Row B shows rotation of a 1 μm long gold nanowire about a similar pivot. We can also create pivots as needed with UV polymerization, as shown in row C. We create a pivot using a 1.5 s exposure of a 375 nm laser (25 W/cm^2) focused to a target location (shown by the green crosshairs), which polymerizes a region of fluid on the surface that is invisible to the camera (panels iv,v). The silver nanowire rotates around this fabricated pivot as shown in frames iii and iv. These polymer pivots can be created anywhere within the device to aid in the manipulation of nanostructures.

We can directly rotate a nanowire without using obstructions by partially immobilizing one of its ends. Figure 3A is a sequence of images that demonstrate this process. First, we position one end of a silver nanowire to the location of the UV focal point (indicated by the green crosshair). A 0.5 s UV exposure (intensity of 90 mW/cm^2) loosely affixes the nanowire to the surface by partially polymerizing the surrounding fluid. The affixed end acts as a pivot about which the nanowire rotates. A subsequent UV exposure at the second wire end permanently immobilizes the wire in place at the desired orientation (see Supporting Information Video si_007). An affixed end allows for 360° rotation of a wire, as shown in Figure 3B (see Supporting Information Video si_008).

dx.doi.org/10.1021/nl402059u | *Nano Lett.* 2013, 13, 3936–3941

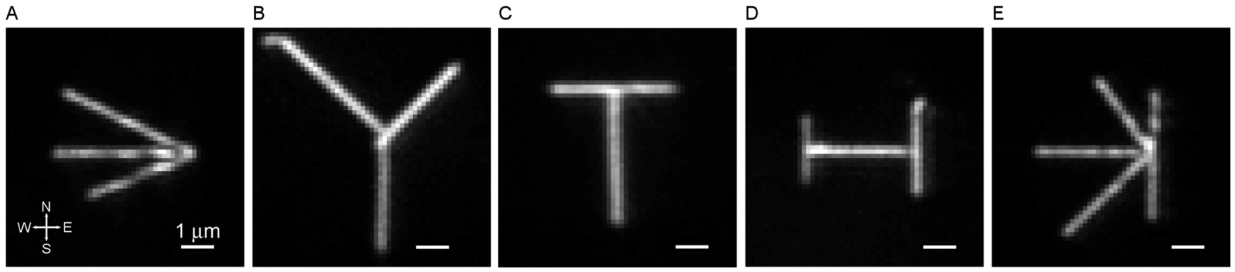

Figure 6. Optical images of silver nanowire nanoassemblies constructed using different combinations of techniques from our fabrication toolbox.

By affixing the end of the silver nanowire we can achieve precise control of its orientation using feedback. The angle of the silver nanowire is measured by performing a least-squares fit of the image to a line.[28] This information is fed back to the controller that continually adjusts flow to hold the wire orientation at the desired angle. We quantify the orientational precision by monitoring the angle of a wire held by feedback for 1 min. The angular standard deviation, correcting for fluctuations in the tracking algorithm, was measured to be σ_θ = 0.4° (see Supporting Information).

To determine the precision with which we can immobilize, we repeat the full procedure illustrated in Figure 3A for 15 silver nanowires. For each nanowire, we immobilize one end, rotate the wire to N−S orientation, and then immobilize the second end. We measure the final orientation of all 15 wires and calculate the differences in angle from the desired orientation. The measured differences have a standard deviation of 0.53°. This standard deviation is close to the measured precision of the control algorithm, which suggests that the immobilization step contributes only a small additional error.

Immobilized nanowires can further enhance manipulation by acting as barriers to separate, combine, and orient moving nanostructures. Figure 4 shows how an immobilized silver nanowire can be used to separate and combine quantum dots (see Supporting Information Videos si_009 and si_010). The silver nanowire and quantum dots are imaged simultaneously using a combination of white light and 532 nm excitation. Figure 4A shows two quantum dots being separated using an immobilized silver nanowire (delineated in green) as a barrier. The figure shows a sequence of time-stamped images, along with an illustration of the approach. Separation uses the end of the nanowire to wedge one quantum dot (circled in blue) apart from the second (circled in red). Figure 4B shows the reverse process, in which we combine two quantum dots by pushing them against a common nanowire barrier. Once combined, the quantum dots can be steered together and positioned to a desired location. These same approaches can be applied to other types of nanostructures.

Figure 5 demonstrates nanostructure orientation using silver nanowire guides and barriers. In Figure 5A, flow is used to align a gold nanowire with a silver nanowire (see Supporting Information Video si_011 and si_012). The silver nanowire serves as a guide to orient the gold nanowire in the parallel direction. Once together, the silver nanowire guides the gold nanowire along its surface (panels iv−v). Immobilized nanowires can also orient mobile nanowires at various relative angles. Figure 5B demonstrates orientation of one silver nanowire using a second immobilized silver nanowire as a barrier. We create a component of the fluid flow normal to the barrier to exert a force that holds one end of the mobile silver nanowire in place by static friction. A parallel flow component rotates it in either direction. Static friction provides ample footing for rotation angles as large as 40° to normal.

As a final demonstration, we use a combination of the techniques from our toolbox to fabricate nanoassemblies from individual silver nanowires, as shown in Figure 6. For each structure, we first immobilize a nanowire either along the E−W direction (panels A and D) or N−S direction (panels B, C, and E) using the technique outlined in Figure 3A. We assemble the subsequent nanowires in panels A−D by first coarsely orienting and placing them near the correct location (the technique in Figure 2, but using the immobilized nanowire ends as pivots). We then achieve finer orientation by tacking down one end of the nanowire and rotating the other. Once oriented, we immobilize the second nanowire end. The nanoassembly pictured in Figure 6E uses the technique shown in Figure 5B to orient a second nanowire perpendicular to the first. We orient subsequent nanowires using the "v"-shaped footholds created by the first two and immobilize them with UV. (See Supporting Information Video si_013 for the assembly in Figure 6E.) Additionally, when required, we use immobilized barriers to separate unwanted nanowires from a desired nanowire (using the technique described in Figure 4A) to perform assembly with these isolated nanostructures.

In conclusion, we have demonstrated a microfluidic approach for creating nanoassemblies on chip with nanoscale precision. We used flow control and an engineered photoresist to position and immobilize a variety of individual nanostructures on a 2D surface. We created a variety of nanoassemblies using combinations of these various capabilities. The ability to assemble metallic nanowires and quantum dots could find application for developing subwavelength interferometers[3] and resonators,[38] single-photon sources,[39] and nonlinear quantum devices.[6] Although this work focused on manipulation of nanophotonic structures, flow control can be used to manipulate a much broader spectrum of objects that include cells, magnetic nanoparticles, and molecules, using a single manipulation platform. Our results could therefore find applications in the study of interacting optical, biological, chemical, and magnetic systems and potentially provide new methods to bridge the gap between these various fields.

■ ASSOCIATED CONTENT

Ⓢ Supporting Information

Determination of the positioning and orienting precision for a silver nanowire and 12 movies. This material is available free of charge via the Internet at http://pubs.acs.org.

■ AUTHOR INFORMATION

Corresponding Author

*E-mail: (E.W.) edowaks@umd.edu; (B.S.) benshap@umd.edu; (J.T.F.) fourkas@umd.edu.

Notes

The authors declare no competing financial interest.

■ ACKNOWLEDGMENTS

This work was supported by a DARPA Defense Science Office grant (Grant W31P4Q0910013). E.W. acknowledges funding support from a National Science Foundation CAREER award (Grant ECCS - 0846494), the Physics Frontier Center at the Joint Quantum Institute (Grant PHY-0822671), and the Office of Naval Research Applied Electromagnetics Center (Grant N000140911190). J.H.S. (gold nanowire synthesis) was supported by the WCU program by the KOSEF under the MEST (Grant R31-2008-000-10071-0)

■ REFERENCES

(1) Cui, Y.; Lieber, C. M. *Science* **2001**, *291*, 851−853.
(2) Engheta, N. *Science* **2007**, *317*, 1698−1702.
(3) Wei, H.; Li, Z.; Tian, X.; Wang, Z.; Cong, F.; Liu, N.; Zhang, S.; Nordlander, P.; Halas, N. J.; Xu, H. *Nano Lett.* **2011**, *11*, 471−475.
(4) Anker, J. N.; Hall, W. P.; Lyandres, O.; Shah, N. C.; Zhao, J.; Van Duyne, R. P. *Nat. Mater.* **2008**, *7*, 442−453.
(5) Fan, J. A.; Wu, C.; Bao, K.; Bao, J.; Bardhan, R.; Halas, N. J.; Manoharan, V. N.; Nordlander, P.; Shvets, G.; Capasso, F. *Science* **2010**, *328*, 1135−1138.
(6) Chang, D. E.; Sørensen, A. S.; Demler, E. A.; Lukin, M. D. *Nat. Phys.* **2007**, *3*, 807−812.
(7) Alivisatos, A. P. *Science* **1996**, *271*, 933−937.
(8) Dickson, R. M.; Lyon, L. A. *J. Phys. Chem. B* **2000**, *104*, 6095−6098.
(9) Akimov, A. V.; Mukherjee, A.; Yu, C. L.; Chang, D. E.; Zibrov, A. S.; Hemmer, P. R.; Park, H.; Lukin, M. D. *Nature* **2007**, *450*, 402−406.
(10) Knight, M. W.; Grady, N. K.; Bardhan, R.; Hao, F.; Nordlander, P.; Halas, N. J. *Nano Lett.* **2007**, *7*, 2346−2350.
(11) Lee, S. Y.; Hung, L.; Lang, G. S.; Cornett, J. E.; Mayergoyz, I. D.; Rabin, O. *ACS Nano* **2010**, *4*, 5763−5772.
(12) Jauffred, L.; Richardson, A. C.; Oddershede, L. B. *Nano Lett* **2008**, *8*, 3376−3380.
(13) Sinclair, G.; Jordan, P.; Courtial, J.; Padgett, M.; Cooper, J.; Laczik, Z. *Opt. Express* **2004**, *12*, 5475−5480.
(14) Yu, T.; Cheong, F.-C.; Sow, C.-H. *Nanotechnology* **2004**, *15*, 1732.
(15) Dawood, F.; Qin, S.; Li, L.; Lin, E. Y.; Fourkas, J. T. *Chem. Sci.* **2012**, *3*, 2449−2456.
(16) Dienerowitz, M.; Mazilu, M.; Dholakia, K. *J. Nanophotonics* **2008**, *2*, 021875.
(17) Amblard, F.; Yurke, B.; Pargellis, A.; Leibler, S. *Rev. Sci. Instrum.* **1996**, *67*, 818−827.
(18) Ramos, A.; Morgan, H.; Green, N. G.; Castellanos, A. *J. Phys. Appl. Phys.* **1998**, *31*, 2338−2353.
(19) Benson, O. *Nature* **2011**, *480*, 193−199.
(20) Sitti, M.; Hashimoto, H. *IEEE/ASME Trans. Mechatronics* **2000**, *5*, 199−211.
(21) Chey, S. J.; Huang, L.; Weaver, J. H. *Appl. Phys. Lett.* **1998**, *72*, 2698−2700.
(22) Ropp, C.; Cummins, Z.; Probst, R.; Qin, S.; Fourkas, J. T.; Shapiro, B.; Waks, E. *Nano Lett.* **2010**, *10*, 4673−4679.
(23) Ropp, C.; Cummins, Z.; Nah, S.; Fourkas, J. T.; Shapiro, B.; Waks, E. *Nat. Commun.* **2013**, *4*, 1447.
(24) Armani, M.; Chaudhary, S.; Probst, R.; Shapiro, B. In *18th IEEE International Conference on Micro Electro Mechanical Systems*, Miami, FL, Jan. 30−Feb. 3, 2005; IEEE: New York; pp 855−858.
(25) Cohen, A. E.; Moerner, W. E. *Proc. Natl. Acad. Sci. U.S.A.* **2006**, *103*, 4362−4365.
(26) Cohen, A. E.; Moerner, W. E. *Opt. Express* **2008**, *16*, 6941−6956.
(27) Ropp, C.; Probst, R.; Cummins, Z.; Kumar, R.; Berglund, A. J.; Raghavan, S. R.; Waks, E.; Shapiro, B. *Nano Lett.* **2010**, *10*, 2525−2530.
(28) Mathai, P. P.; Carmichael, P. T.; Shapiro, B. A.; Liddle, J. A. *RSC Adv.* **2013**, *3*, 2677−2682.
(29) Armani, M. D.; Chaudhary, S. V.; Probst, R.; Shapiro, B. *J. Microelectromech. Syst.* **2006**, *15*, 945−956.
(30) Probstein, R. F. *Physicochemical Hydrodynamics*; John Wiley and Sons: New York, 1994.
(31) Thompson, R. E.; Larson, D. R.; Webb, W. W. *Biophys. J.* **2002**, *82*, 2775−2783.
(32) Kumar, R.; Raghavan, S. R. *Langmuir* **2010**, *26*, 56−62.
(33) Kumar, R.; Kalur, G. C.; Ziserman, L.; Danino, D.; Raghavan, S. R. *Langmuir* **2007**, *23*, 12849−12856.
(34) Kojima, K.; Ito, M.; Morishita, H.; Hayashi, N. *Chem. Mater.* **1998**, *10*, 3429−3433.
(35) Sun, Y.; Yin, Y.; Mayers, B. T.; Herricks, T.; Xia, Y. *Chem. Mater.* **2002**, *14*, 4736−4745.
(36) Friese, M. E. J.; Nieminen, T. A.; Heckenberg, N. R.; Rubinsztein-Dunlop, H. *Nature* **1998**, *394*, 348−350.
(37) Sacconi, L.; Romano, G.; Ballerini, R.; Capitanio, M.; De Pas, M.; Giuntini, M.; Dunlap, D.; Finzi, L.; Pavone, F. S. *Opt. Lett.* **2001**, *26*, 1359−1361.
(38) Ditlbacher, H.; Hohenau, A.; Wagner, D.; Kreibig, U.; Rogers, M.; Hofer, F.; Aussenegg, F. R.; Krenn, J. R. *Phys. Rev. Lett.* **2005**, *95*, 257403.
(39) Chang, D. E.; Sørensen, A. S.; Hemmer, P. R.; Lukin, M. D. *Phys. Rev. Lett.* **2006**, *97*, 053002.

Fabrication of Nanoassemblies Using Flow Control

Chad Ropp,[†] *Zachary Cummins,*[‡] *Sanghee Nah,*[§] *Sijia Qin,*[§] *Ji Hyun Seog,*[⊥] *Sang Bok Lee,*[⊥,§] *John T. Fourkas,*[*,§,¶] *Benjamin Shapiro,*[*,‡] *Edo Waks,*[*,†]

[†]Department of Electrical and Computer Engineering / IREAP, [‡]Fischell Department of Bio-Engineering, [§]Department of Chemistry and Biochemistry, and [¶]Institute for Physical Science and Technology, University of Maryland, College Park, Maryland 20742, United States [⊥]Graduate School of Nanoscience and Technology (WCU), KAIST, 335 Gwahak-ro, Yuseong-Gu, Daejeon, 305-701, Korea

Supporting Information

We determine the precision for positioning a silver nanowire by holding a single nanowire in place and continuously monitoring its position. Figure S1A is a scatter plot of the held nanowire positions, which are rotated so that the *x* (*y*) coordinate correspond to the direction perpendicular (parallel) to the wire axis. Figures S1B and S1C are histograms of the positions for each coordinate. The standard deviation in held position is σ_{hp} = 6 (4) nm in the directions perpendicular (parallel) to the wire axis. We perform the same measurement using a silver nanowire that is adhered to the surface to determine the precision of the tracking algorithm. We determine the uncertainty in tracking the wire position to be σ_{tp} = 3 (2) nm in the perpendicular (parallel) directions. The positioning precision is calculated by subtracting tracking uncertainty from the held position precision using $\sigma_p = \sqrt{\sigma_{hp}^2 - \sigma_{tp}^2}$, which yields $\sigma_p = 5$ (3) nm perpendicular (parallel) to the wire.

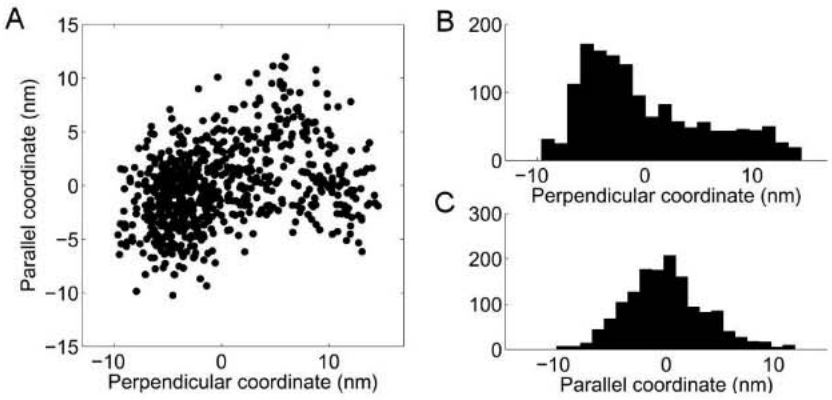

Figure S1 A. Scatter plot of the measured centroid location of a nanowire held in place by flow control Histograms of the measured positions in the direction (B) perpendicular and (C) parallel to the wire axis.

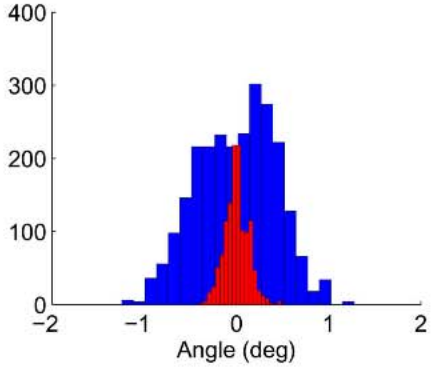

Figure S2 Histograms comparing the measured angle of a silver nanowire that is immobilized on a surface (red) with one that is oriented by flow control (blue)

Affixing one end of a silver nanowire to the surface with polymer provides precise control of the nanowire's orientation. We quantify orientational precision by monitoring the angle of a wire held by feedback for 1 minute. Figure S2 plots histograms of the measured angles for the held wire (blue) compared to the measured angle for an immobile silver nanowire (red). We calculate the standard deviation in held angle, $\sigma_{h\theta} = 0.42°$. The standard deviation of the immobilized nanowire's angle provides an estimate for the uncertainty in tracking the wire's angle, determined to be $\sigma_{t\theta} = 0.13°$. We subtract the tracking uncertainty from the held angle precision to calculate the orientation precision given by $\sigma_\theta = \sqrt{\sigma_{h\theta}^2 - \sigma_{t\theta}^2}$ which is calculated to be 0.40°.